



Marine Heat waves – Multiple Analysis /
Definitions (MHW-MAD): A Multi-Definition
Global Marine Heatwave Dataset from
Satellite Sea Surface Temperature data

5 Authors:

- 6 Alex Hayward¹, Nishka Dasgupta¹, Ronan McAdam², Mark R. Payne¹, Roshin Raj³, Giulia
- 7 Bonino², Sourav Chatterjee⁴, Vincent Combes⁵, Dimitra Denaxa⁶, Francesco De Rovere², Pia
- 8 Englyst¹, Veera Haapaniemi⁻, Paul Hargous⁵, Jacob Høyer¹, K Ajith Joseph®, Beatriz Lopes®,
- 9 Ana Olivieraº, João Paixãoº, Fabiola Silvaº, Saradhy Surendrane, Artemis Zegna-Rata¹o,
- 10 Steffen Olsen¹

11 Affiliations:

- 12 ¹ Danish Meteorological Institute (DMI), Copenhagen, Denmark
- 13 ² CMCC Foundation Euro-Mediterranean Centre on Climate Change, Bologna, Italy
- 14 3 Nansen Environmental and Remote Sensing Center (NERSC), Bergen, Norway
- 15 A National Centre for Polar and Ocean Research (NCPOR), Goa, India
- 16 5 Spanish National Research Council (CSIC), Spain
- 17 6 Hellenic Centre for Marine Research (HCMR), Athens, Greece
- 18 ⁷ Finnish Meteorological Institute (FMI), Helsinki, Finland
- 19 8 Nansen Environmental Research Centre India (NERCI), Kochi, India
- 20 9 +ATLANTIC CoLAB, Matosinhos, Portugal
- 21 10 Laboratoire de Météorologie Dynamique (LMD), Paris, France

22

23 Corresponding author: Alex Hayward algh@dmi.dk

24 Abstract

25 Marine heatwaves (MHWs) are prolonged anomalies of warm sea surface temperature 26 (SST) that can disrupt marine ecosystems, physical climate processes, and human coastal 27 activities. MHW definitions vary due to different stakeholders requirements, such as 28 ecological scientists and climate scientists having differing yet specific thresholds and 29 metrics. Here we introduce a new global dataset of daily MHW metrics: climatological 30 baselines, threshold exceedances, SST anomalies, and categorical event classifications of 31 severity, derived from the European Space Agency SST Climate Change Initiative (ESA SST 32 CCI) climate data record (CDR; 1982-2021) version 3.0 and an extension from 2022-2024 33 provided as an interim climate data record (iCDR). Building on the widely used definition of 34 MHWs, periods in which SST exceeds the local 90th percentile for 5 or more days, our 35 dataset extends this framework by incorporating multiple baseline climatologies (including 36 fixed 30-year periods and rolling 30-year windows, as well as the period for reanalysis 1993 -





37 2016), varied percentile thresholds (90th, 95th, 99th), and both raw and linearly detrended SST anomalies. We also implement alternative event duration criteria (minimum 10-day and 30 30-day persistence) to classify longer-lasting warm events. All data products are provided at 40 daily resolution on a 0.05° (~5 km) grid, with outputs including daily climatological 41 percentiles, SST anomalies and binary MHW flags with severity category indices. This 42 comprehensive dataset provides a consistent foundation for detecting and analysing MHWs 43 across time and space, enabling researchers to assess how methodological choices affect 44 MHW characterisation. By offering multiple definitions in parallel, the dataset facilitates 45 intercomparison studies and supports applications from climate monitoring and model 46 evaluation to marine ecological impact assessment, thereby providing users with pre-made 47 indices for extremes.

1.Introduction

49 Marine heatwaves (MHWs) are discrete, prolonged periods of abnormally high ocean 50 temperatures relative to typical local conditions (Hobday et al., 2016). They often persist for 51 days to months and can extend over vast regions (>1000 km). MHWs can have important 52 ecological and socioeconomic impacts. For example, extreme warming events have caused 53 mass mortalities of marine organisms and biodiversity loss, including coral bleaching events 54 (Garrabou et al., 2019; Hsu et al., 2025), harmful algal blooms (Roberts et al., 2019), shifts 55 in species distributions (Lonhart et al., 2019), and declines in fisheries (Wernberg et al., 56 2016; Smale et al., 2019; Gonzalez et al., 2025). Demonstrating these effects, an intense 57 MHW off Western Australia in 2011 removed ~100 km of kelp forests (~90% of the region's 58 kelp), leading to a regime shift in the local ecosystem (Wernberg et al., 2016). Such events 59 threaten the resilience of marine ecosystems and the services they provide to coastal 60 communities.

61 There is clear evidence that the frequency and intensity of MHWs are increasing under 62 climate change (Frolicher et al., 2019; Lien et al., 2023). Long-term analyses indicate that 63 from 1925 to 2016, the average annual number of MHW days has increased globally by over 64 50% (Oliver et al., 2018). In recent decades, many MHW events have been attributed to 65 anthropogenic warming (Oliver et al., 2018; Smale et al., 2019), and are expected to 66 increase in frequency by the end of the century (Frolicher et al., 2019). In particular, the 67 duration and spatial extent of MHWs have expanded, coincident with the rise in baseline 68 ocean temperatures. These trends underscore the urgency of monitoring MHWs as well as 69 understanding their drivers.

70 Despite growing research, there is still ongoing debate on how best to define and detect T1 MHWs across different studies (Farchadi et al., 2025; Smith et al., 2025), with the most T2 common definition taken from Hobday et al., (2016). How MHWs are identified depends on T3 methodological choices including the baseline climatology period, threshold percentiles, and T4 minimum duration, among other factors. Some studies use a fixed historical baseline (e.g. T5 30-year climatology) whereas others use a shifting baseline that moves with each year. In a T6 warming climate, a fixed baseline (such as the standard World Meteorological standard T7 30-year baseline between 1991 to 2020) will likely label more recent warm events as T8 extreme (Oliver et al., 2018) compared to a moving baseline (or periodically updated T9 "normal"). A shifting baseline effectively raises the threshold over time, filtering out the





80 warming (or cooling) trend and highlighting interannual variability. Similarly, choosing a 90th s1 percentile threshold versus a more extreme 95th or 99th percentile can substantially change which events qualify as MHW. The required duration matters as well too; the original Hobday et al. (2016) definition requires ≥5 consecutive days, but some applications consider longer minima (e.g. 10 days or more) to isolate only the most persistent events. Due to the vast array of methodological differences, recent studies have called for clearer and more standardised MHW definitions to aid comparisons and decision-making (Amaya et al., 2023; Farchadi et al., 2025).

88 To address these differences, we present a "multi-definition" global MHW dataset that allows 89 users to examine events under a suite of definitions within a single, consistent framework. 90 We derive this dataset from the European Space Agency SST Climate Change Initiative 91 (ESA SST CCI) Climate Data Record (CDR) v.30 (Embury et al., 2024), which combines 92 data from different satellite sensors into a daily 0.05° gridded gap-free SST product (in the 93 future we plan to incorporate more SST products).

94 The MHW dataset provides multiple climatological baselines (both a fixed 30-year baseline 95 and rolling 30-year windows) so that users can explore the influence of baseline period on 96 detected MHWs. We include both raw and detrended SST anomaly fields, enabling analysis 97 of MHWs with and without the long-term warming signal. Furthermore, we provide event 98 detections based on the standard 90th-percentile/5-day definition, but also on more stringent 99 threshold exceedances (95th and 99th percentiles) and longer minimum durations (10-day 100 and 30-day). By offering these options side-by-side, the dataset facilitates comparative 101 studies of how MHW properties change under different definition choices. In the following, 102 we describe the data sources and processing methods, present example results comparing 103 definitions including a case study of the 2014 "Blob" event in the Northeast Pacific (Bond et 104 al., 2014), an unusually large and persistent MHW (2013-2016) that disrupted ecosystem 105 processes, causing mass mortalities (Renner et al., 2024). Further to this, we detail data 106 availability and potential uses, and examine the broader implications of this multi-definition 107 approach.

2. Sea Surface Temperature Data

109 The ESA SST CCI CDR v3.0 CDR and ICDR are based on the same software and systems, 110 which ensures a consistent and uninterrupted daily global SST time series covering the 111 years 1982 through 2025. In this study, the Level 4 (L4) analysis product is used, which 112 combines SST observations from multiple satellite instruments into a daily gridded gap-free 113 product at 0.05°x 0.05° resolution. The L4 analysis product integrates infrared and 114 microwave sensor SST retrievals from 22 different satellite missions (Embury et al., 2024). 115 The infrared and microwave signals were collected from the following four series of sensors: 116 15 Advanced Very High Resolution Radiometers (AVHRRs), three Advanced Along-Track 117 Scanning Radiometers ((A)ATSR), two Sea and Land Surface Temperature Radiometer 118 (SLSTR) and two Advanced Microwave Scanning Radiometers (AMSRs). The L4 analysis 119 product is produced using the climate configuration of the Operational Sea Surface 120 Temperature and Ice Analysis (OSTIA) system (Donlon et al., 2012; Good et al., 2020), 121 which blends the input SST data from multiple satellite sensors and corrects for diurnal 122 warming and depth-based temperature gradients, by standardising SST values to ~20 cm





4

123 depth. Unlike the OSTIA reprocessed L4 dataset (Good et al., 2020), the ESA SST CCI 124 system does not assimilate in situ data into its L4 product, thereby preserving 125 satellite-derived trends.

126 The ESA SST CCI CDR v3.0, is specifically designed for robust climate research through 127 rigorous inter-sensor calibration and bias corrections (Embury et al. 2024). As a result, the 128 physics-based retrieval algorithms generate a stable, low-bias SST dataset that is largely 129 independent of in situ observations. The CCI SST L4 SST product adheres to Group for High 130 Resolution SST (GHRSST) standards, delivering daily, gap-free global SST fields ideal for 131 the assessment of MHWs (Yang et al., 2021). Furthermore, the SST CCI v3.0 has been 132 proven as a suitable product for long-term ocean climate studies, including the detection and 133 characterisation of MHWs (Yang et al., 2021). This being said, the approach taken can be 134 implemented on different SST products and algorithms, and we hope to explore this in the 135 future.

3. Marine Heatwave Definitions and Framework

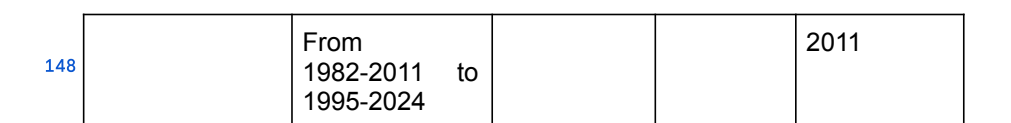
137 Definitions of MHWs were selected and assessed, based on percentiles, baselines, 138 persistence, and detrended data. All data processing was performed using Python and 139 Climate Data Operators (CDO) software 2.1.1, with some of the post-processing also done 140 with the help of NCO 5.2.1. We first computed long-term climatologies for each grid cell and 141 day-of-year (DOY) using multiple baseline definitions (Fig. 1). We then calculated daily SST 142 anomalies relative to those climatologies and identified MHW events by applying threshold 143 criteria to the anomaly time series, as in Hobday et al., (2016). We then categorised the 144 intensity of detected events using the severity index of Hobday et al., (2018) and organised 145 all output variables into CF compliant NetCDF files, for 10 different sets of definitions (Fig. 1; 146 Table. 1). All the framework steps are described in detail in the following paragraphs.

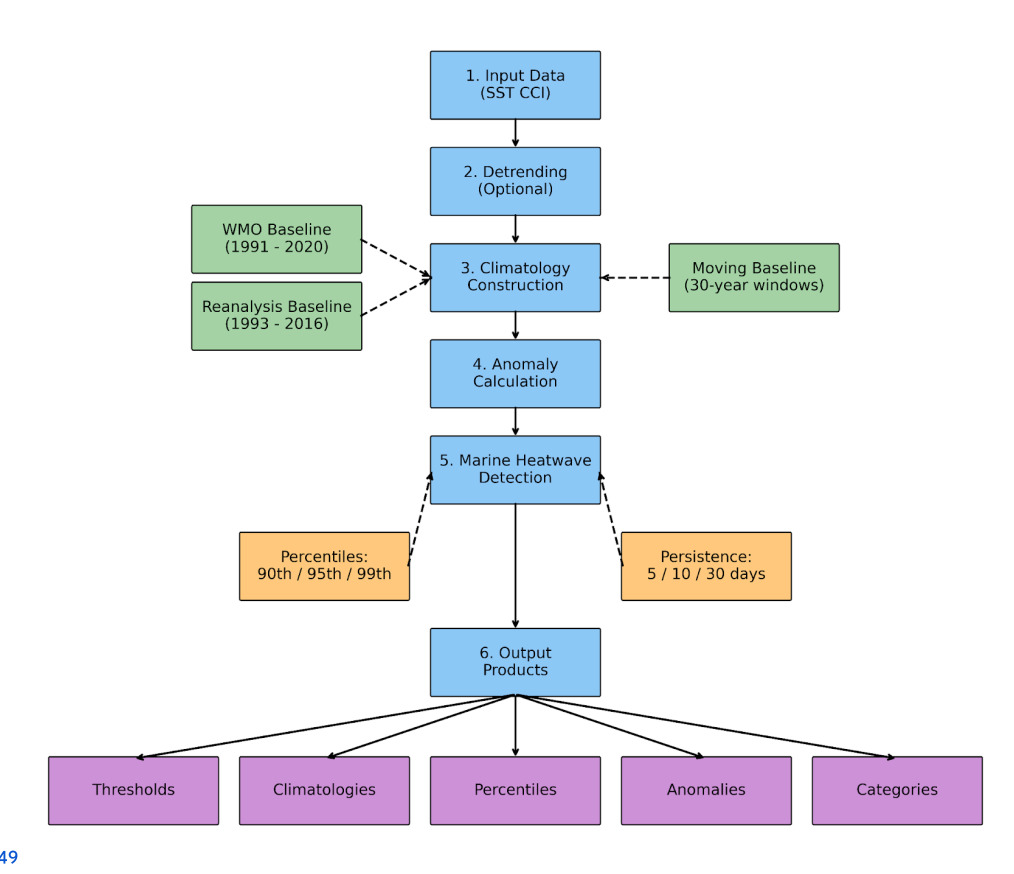
147 **Table 1.** Definitions used to build the MHW-MAD dataset

Definitions	Baseline Period	Percentiles	Min. Duration (days)	Notes
WMO (percentiles)	1991-2020	90th, 95th, 99th	5	
Reanalyses period	1993-2016	90th, 95th, 99th	5	
Persistence	1991-2020	90th	10, 30	
Detrended	1991-2020	90th	5	Detrend SST (calendar day)
Moving	30 year moving*	90th	5	*MHWs starting from









150 Figure 1: Workflow for creating daily MHW metrics based on different definitions.

151 3.1 Detrending of SST Time Series

152 Long-term ocean warming elevates the baseline SST over time for most areas, causing 153 more frequent MHW events in later years if the baseline remains static. To allow users to 154 separate the effect of global warming from natural variability, we created a detrended version 155 of the SST record. In areas without strong decadal variability, removing the trend ensures 156 that the baseline climatology represents the stationary seasonal cycle, so that anomalies 157 and MHW detections reflect short-term fluctuations rather than the slowly shifting mean 158 (Schlegel et al., 2019). This approach can be useful for attribution studies, as MHW 159 occurrence after detrending can be interpreted as the portion driven by natural variability 160 without the influence of long-term climate warming.

161 We applied a grid-point-specific linear detrending to the SST time series for each calendar 162 day-of-year. For each grid cell, all SST values corresponding to the same calendar date





163 across 1982–2024 were collated (e.g., all January 15 values over the 44-year span). We 164 then performed an ordinary least squares linear regression of SST against the year for each 165 calendar date at each grid cell. This yields a linear warming (or cooling) rate for that date 166 and location (Fig. 2). The linear trend component for a given day was then subtracted from 167 the original SST value. Detrending was applied at all grid cells regardless of statistical 168 significance to ensure the dataset remained gap-free. The result is a parallel SST dataset 169 where each grid cell's time series has no linear trend over 1982–2024. It is important to note 170 that the detrending was only undertaken for the standard Hobday MHW definition of 171 exceedance of the 90th percentile, 5-day persistence, and WMO climatology (1991–2020).

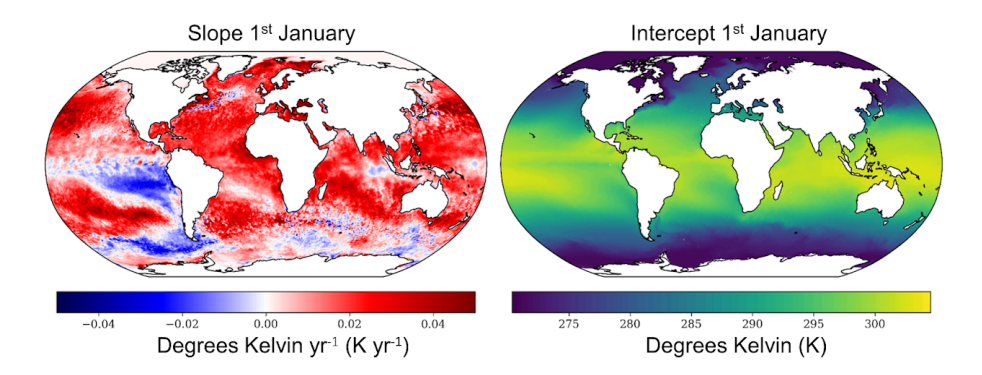


Figure 2. The slope and intercept used for detrending SST CCI data. The example shown is 174 for the first of January.

175 3.2 Climatology Construction

176 We defined the climatological baseline as the distribution of SST for each DOY at each grid 177 point, against which anomalies and extremes are measured. Two approaches were used to 178 construct climatologies:

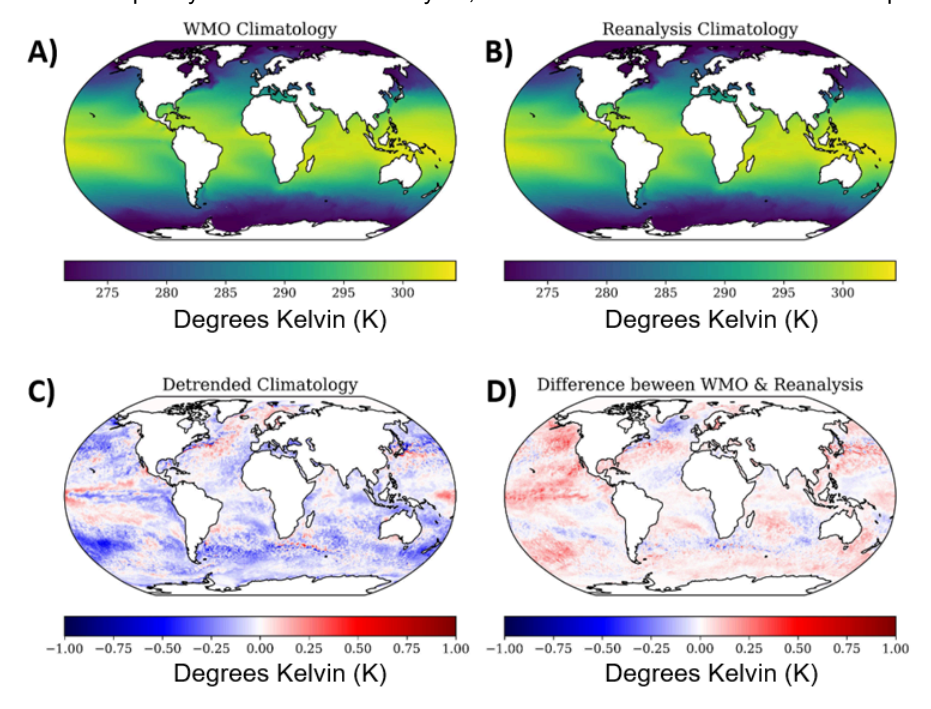
179 (a) Fixed 30-year climatology and reanalysis: We adopted the 30-year period 1991–2020 180 as a representative modern baseline, consistent with WMO-recommended climate normal 181 periods - and hereby refer to this as the 'WMO baseline' (Fig. 3). For day (DOY 1–366) in all 182 baseline periods, we aggregated all SST values for that same DOY, including the 29th 183 February across the 30 years. This yielded, for each grid cell and each DOY, a distribution of 184 30 values (one from each year). From this distribution, we computed the 10th percentile, 185 50th percentile, 90th percentile, and additionally the 95th and 99th percentiles of SST. To 186 ensure smoother day-to-day continuity in the climatology while retaining sensitivity to 187 short-term extremes, we applied a 21-day moving average (wrapped from 31st December to 188 1st January, when required) to the percentile time series as a function of DOY, instead of the 189 30-day window used by Hobday et al. (2016). This shorter smoothing window preserves 190 more of the variability associated with extreme events, which may otherwise be weakened 191 by a longer averaging period. This moderate temporal smoothing (±10 days around each 192 date) reduces sampling noise and prevents abrupt jumps in the threshold from one day to 193 the next, at the cost of slightly blunting the most short-lived seasonal extremes. The same





194 approach was taken for the reanalysis period, however the baseline was instead between 195 1993-2016.

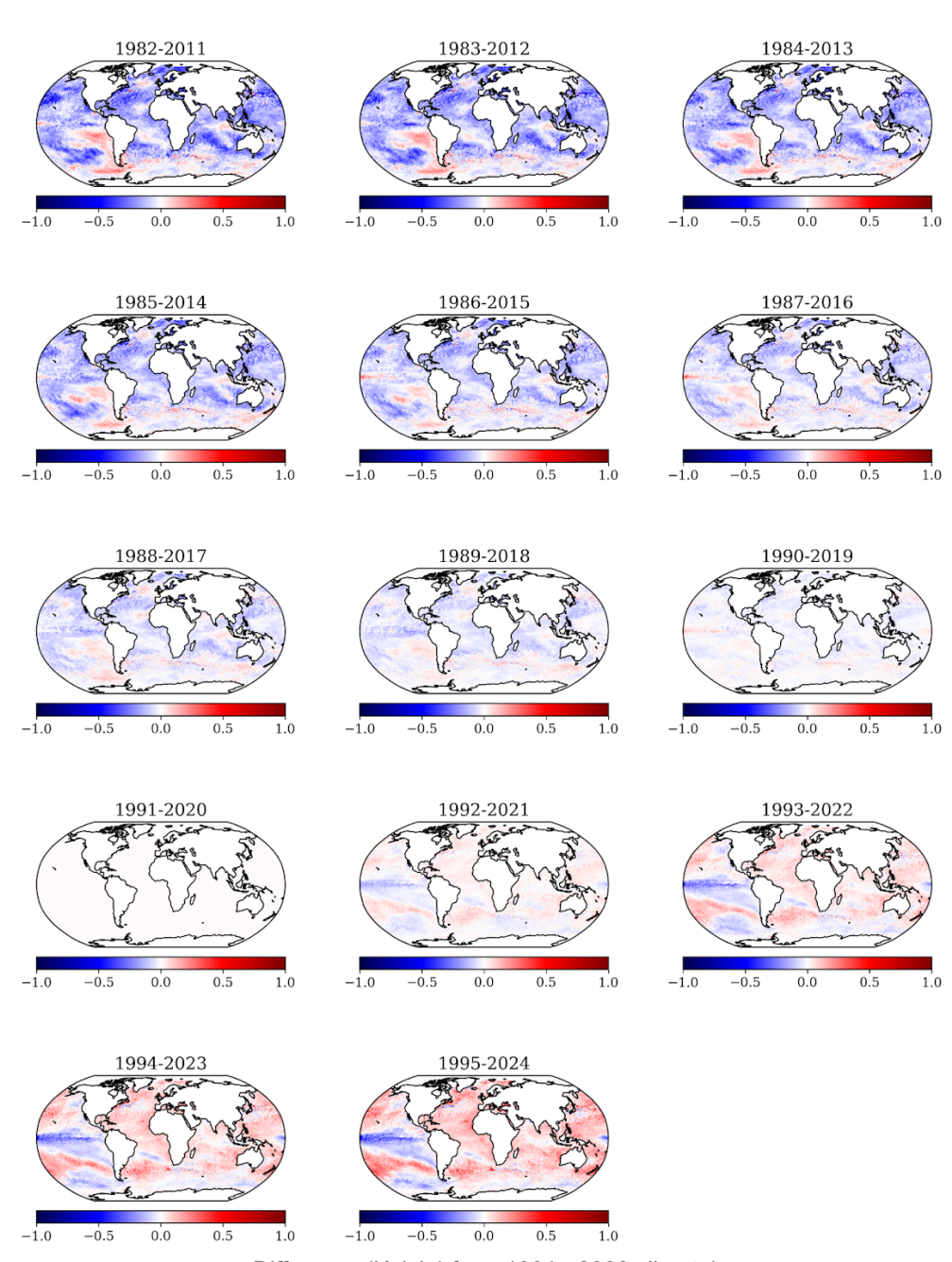
196 (b) Moving 30-year climatology: As the ocean's climate is non-stationary, and warming has 197 been prevalent over the past decades, we computed a series of moving-window 198 climatologies. Starting with the earliest period of 1982–2011, we then advanced the 30-year 199 window by one year at a time (i.e. 1983–2012, 1984-2013... up to 1995–2024). For each 200 window, we calculated daily percentiles using the same method detailed above. The result is 201 a time-evolving climatology that gradually warms (or cools) in most areas over time (Fig. 4). 202 As a consequence of a shifting baseline, extreme anomalies are measured relative to the 203 local contemporary climate for each year, rather than a historical reference period.



205 **Figure 3:** Different climatologies, including: A) WMO climatology (1991–2020), B) 206 Climatology based on the reanalysis period (1993–2016), C) Climatology based on 207 detrended data for the WMO period, and D) Difference between the WMO climatology and

208 the climatology based on the reanalysis period.





Difference (Kelvin) from 1991 - 2020 climatology

210 **Figure 4:** 30-year moving climatologies from 1982-2011 to 1995-2024, based on the WMO 211 definition. Each panel shows the difference to the WMO 1990-2021 climatology for the 1st 212 January for each respective period.





213 3.3 Anomaly Calculation

214 For each day in the record, we calculated SST anomalies as the deviation from the 215 climatology on that DOY. Let SST_x denote the daily sea surface temperature (SST) at a 216 given DOY (x), and M_x the 50th percentile climatology for that DOY. The anomaly is then 217 defined as: anomaly = $SST_x - M_x$.

218 In the anomaly calculations, we used a 366-day reference that explicitly includes 29 219 February. To ensure consistency in non-leap years, all days after 28 February were shifted 220 forward by one in their day-of-year index (i.e. 1 March becomes DOY 61, 2 March DOY 62, 221 and so on). This adjustment preserves the one-to-one correspondence between calendar 222 days and the 366-day climatological reference, ensuring that anomalies for non-leap years 223 are correctly aligned with those from leap years, while avoiding any artificial discontinuities 224 around late February and early March. Anomalies were calculated independently using the 225 fixed-baseline, moving-baseline, and also for the raw and detrended SST data records. 226 These daily anomaly fields form the basis for MHW detection. Positive anomalies indicate 227 warmer-than-normal conditions; negative anomalies indicate colder-than-normal conditions 228 (i.e. used to detect cold spells).

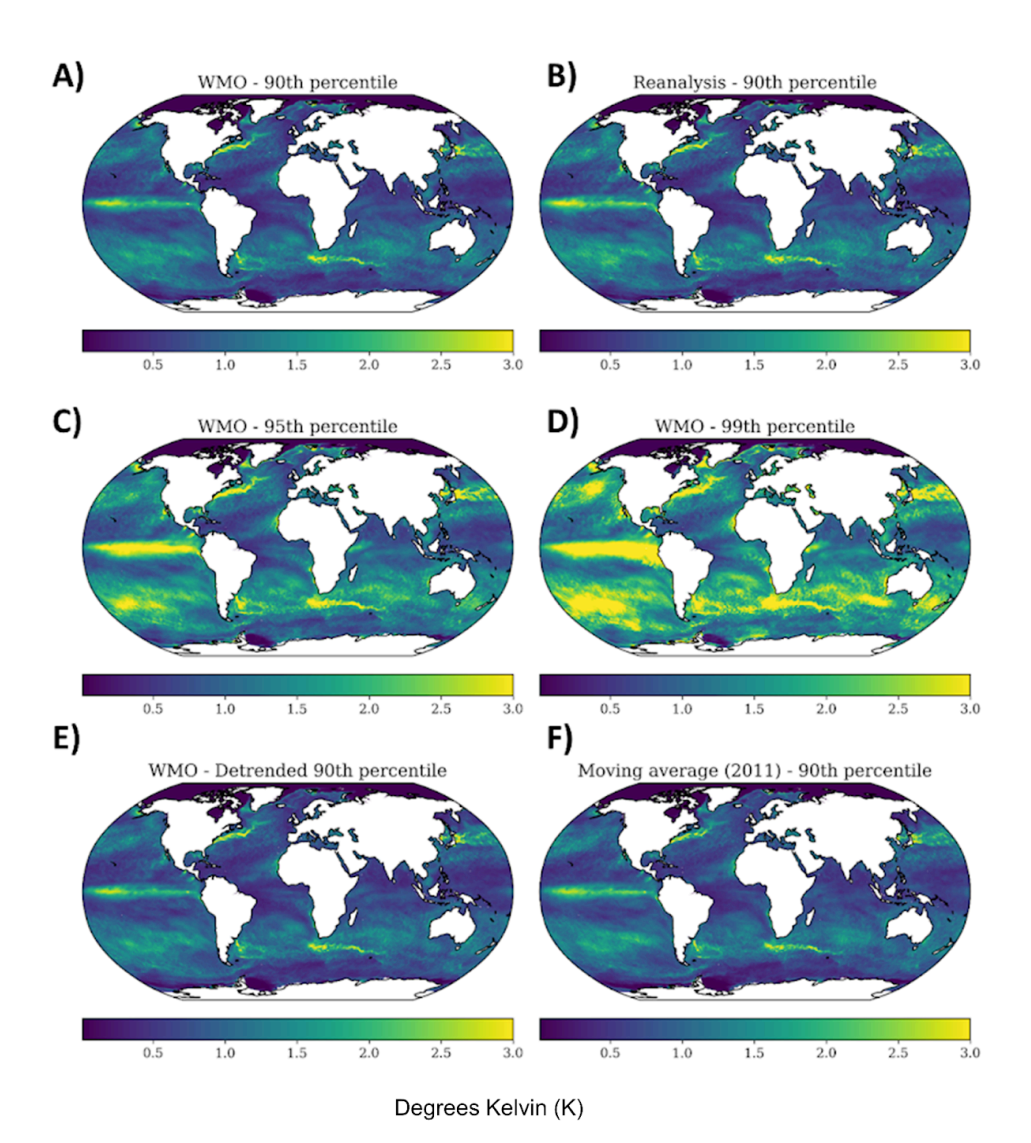
229 3.4 MHW Event Detection

230 MHW events were identified by applying the threshold criteria to the SST anomalies.
231 Following the framework of Hobday et al. (2016), an MHW is detected at a given grid cell
232 whenever the SST (anomaly) exceeds a threshold (90th, 95th or 99th) for a minimum
233 duration of five days (or more). This yields a binary MHW mask indicating the
234 presence/absence of an MHW at each grid cell each day. We implemented multiple
235 threshold and duration combinations:

236 **Extended thresholds:** In addition to the 90th percentile from Hobday's definition, we also 237 used 95th and 99th percentile thresholds (Fig. 4). These higher thresholds capture the more 238 extreme temperature anomalies. Using the 95th or 99th percentile substantially reduces the 239 number of events detected, focusing on the upper tail of extreme warm events. By 240 comparing results from 90th vs. 95th vs. 99th percentile criteria, users can gauge the 241 sensitivity of MHW statistics to the extremeness of the threshold.

242 **Extended persistence criteria:** We also include longer minimum durations for MHWs. We 243 required events to last at least 10 consecutive days above the threshold (instead of 5). We 244 also created another more extreme criteria, where 30 days of consecutive exceedance were 245 required. Naturally, imposing a longer duration criterion filters out shorter temperature 246 anomalies. The 30-day criterion is more restrictive and captures only the most prolonged 247 marine heatwave episodes. These longer-duration definitions can be useful for focusing on 248 events likely to have consequential physical or ecological impacts.

249 **Event metrics:** We have provided the day-by-day anomaly values and threshold 250 exceedance status (Fig. 4), along with severity category (see section 2.5), so users can 251 examine the temporal evolution of each event. Here, we do not assign spatial extents or 252 track contiguous areas of MHW, though such analyses could be done using this dataset.



254 **Figure 5:** Marine heat wave anomaly threshold values (DOY=1) based on different criteria 255 using for the first January. A) the WMO climatology and 90th percentile threshold, B) the 256 reanalysis period (1993 - 2016) and a 90th percentile threshold, C) the WMO climatology 257 with the 95th percentile threshold, D) the WMO climatology with the 99th percentile 258 threshold, E) the detrended data with a 90th percentile threshold, and F) the moving average 259 centred at 2011, with the 90th percentile threshold.

260 **Ice-covered regions:** In areas of sea ice cover, the SST-CCI product provides a value 261 corresponding to the assumed freezing point of sea water of about -1.8°C (assuming 262 salinities of ~33PSU). As a result, areas of multi-year sea ice cover have threshold values of 263 0 (Fig. 4). As both the Arctic and Antarctic have witnessed pronounced sea ice loss in recent 264 times (Stroeve et al., 2007; Purich and Doddridge., 2023), new areas of open water would





265 be classified as marine heat wave hot spots due to their low thresholds, making ecological 266 assessments of SST in polar regions challenging (Hayward et al., 2025, Pecuchet et al., 207 2025). To study polar regions, we suggest using targeted products such as the dedicated 268 Arctic product produced in Copernicus Marine Service (CMEMS), L4 Arctic Ocean - Sea and 269 Ice Surface Temperature Analysis (SST/IST; Nielsen-Englyst et al. 2023) or for Antarctic 270 applications the C3S global L4 SST/IST product produced by the Danish Meteorological 271 Institute (DMI), which in both cases provide satellite-observed sea-ice surface temperatures 272 in sea ice covered areas, and blends the SST and IST observations in the marginal ice 273 zones. MHW analyses based on these products have not been included here.

274 3.5 Categorical Severity Index

275 In addition to the binary identification of MHW days, we also provide a categorical severity 276 index following the approach of Hobday et al. (2018) for classifying MHW intensity levels. 277 Specifically, we define four categories of MHW intensity at each grid cell and day by 278 comparing the SST anomaly to the local threshold difference.

- 279 1. Category 1 ("moderate") corresponds to anomalies just above the threshold (anomaly
 ≥ threshold and <2 times threshold difference),
- 281 2. Category 2 ("strong") for anomalies 2-3 times the threshold difference,
- 3. Category 3 ("severe") for 3-4 times, and
- 4. Category 4 ("extreme") for anomalies ≥4 times the threshold difference.

These provide a simplified way to communicate the severity of an ongoing MHW. We compute such categories for each threshold definition (e.g., 90th, 95th, or 99th percentile) as separate files; a category 4 event for the 99th percentile threshold would only capture very extreme events, indicating using severity indices could also be a good way to track more extreme events instead of higher percentile thresholds.

289 In the dataset, days with no MHW are given a category value of 0. We note that cold spells 290 are not explicitly categorised in this study, however, using this dataset it is possible to 291 classify cold extremes below the 10th percentile.

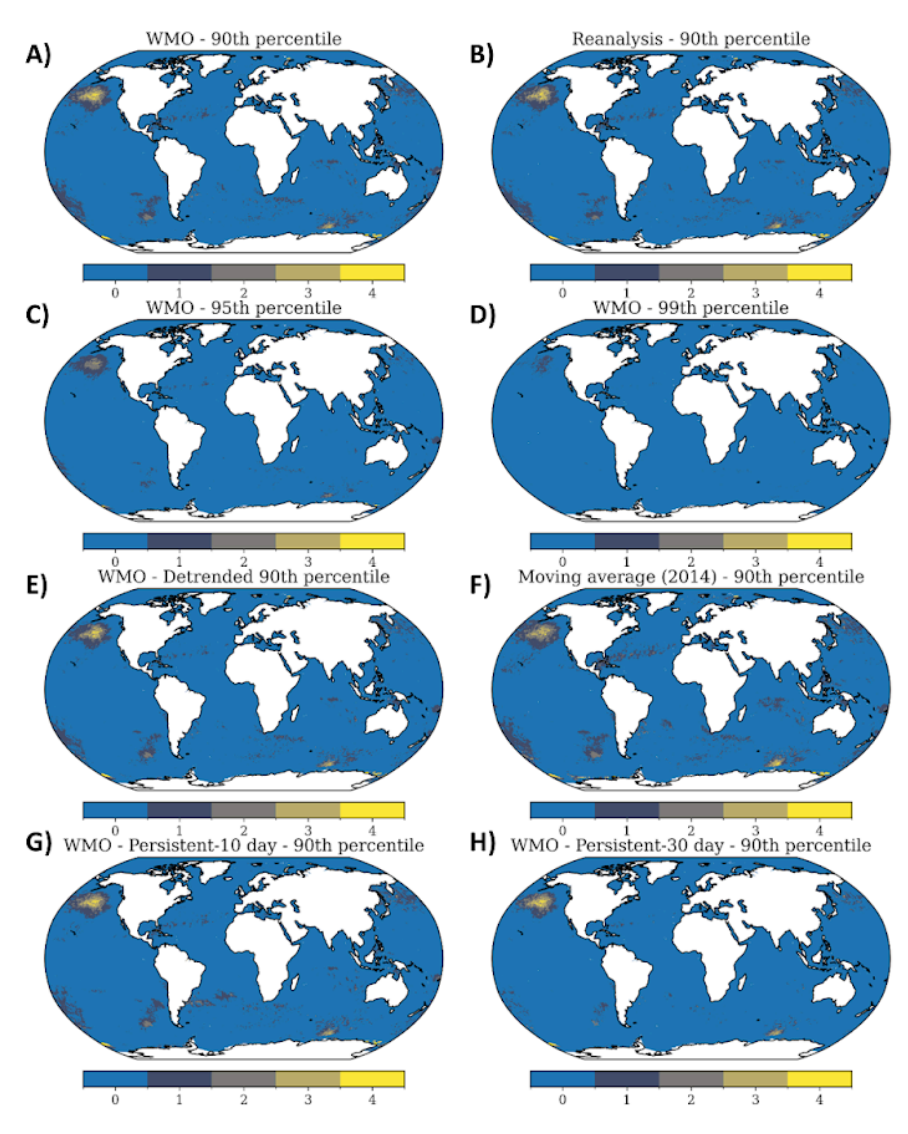


Figure 6: Categories of marine heat waves on 1st January 2014 (during 'the Blob' event) using different definitions. Where A) uses the WMO climatology (1991 to 2020) and the 90th percentile, B) uses the reanalysis period (1993 - 2016) and the 90th percentile, C) uses the WMO climatology and the 95th percentile, D) uses the WMO climatology and the 99th percentile, E) uses the WMO climatology and the 90th percentile with detrended data, F) uses a climatological period between 1985 and 2014, and the 90th percentile, G) uses the WMO climatology and the 90th percentile with a 10 day persistence window, and H) uses the WMO climatology and the 90th percentile with a 30 day persistence window.

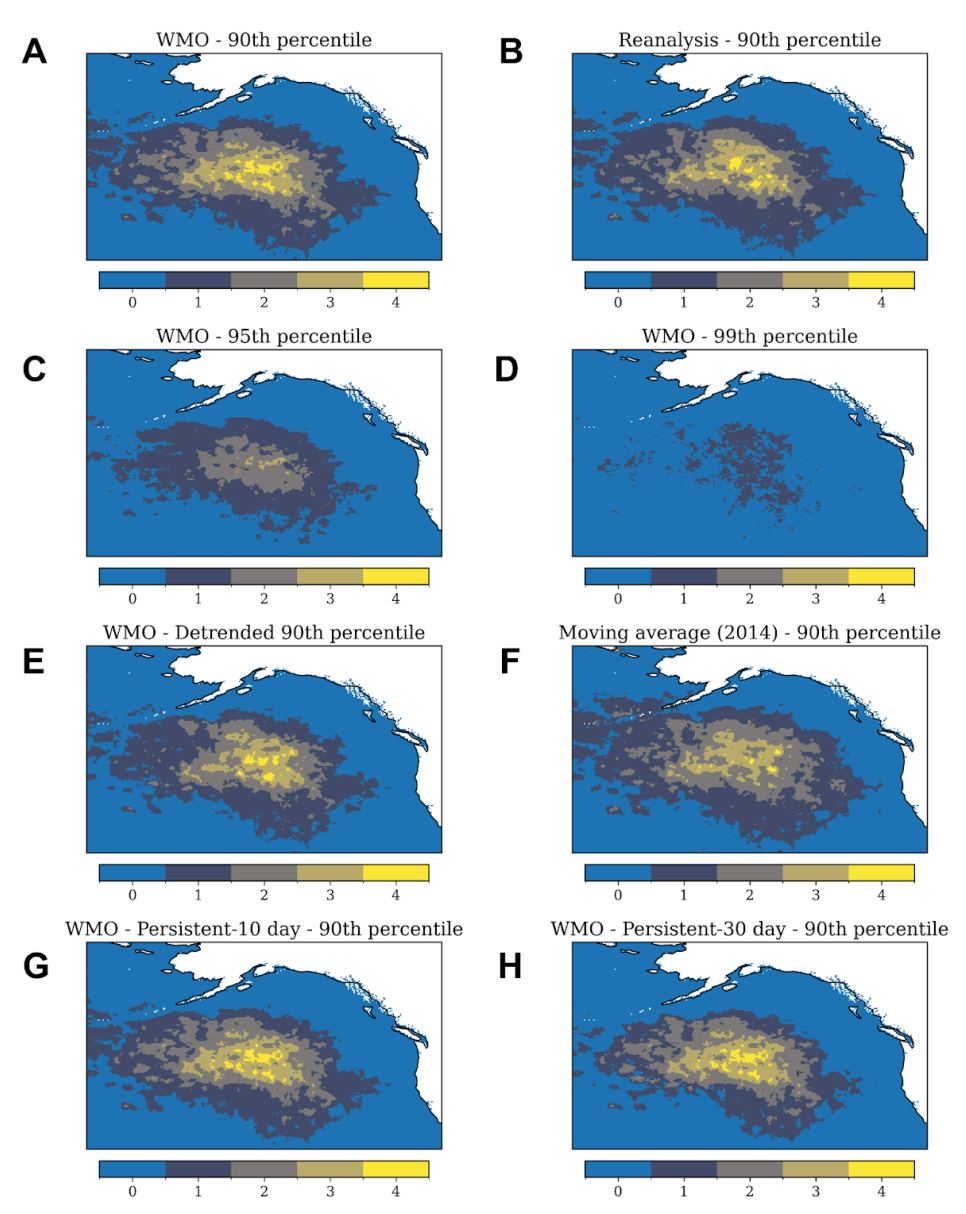


Figure 7: The Pacific Blob on the 1st January 2014 using various definitions. Where A) uses 303 the WMO climatology (1991 to 2020) and the 90th percentile, B) uses the reanalysis period 304 (1993 - 2016) and the 90th percentile, C) uses the WMO climatology and the 95th percentile, 305 D) uses the WMO climatology and the 99th percentile, E) uses the WMO climatology and the 306 90th percentile with detrended data, F) uses a climatological period between 1985 and 2014, 307 and the 90th percentile, G) uses the WMO climatology and the 90th percentile with a 10 day 308 persistence window, and H) uses the WMO climatology and the 90th percentile with a 30 day 309 persistence window.





310 4. Results

311 Below we briefly discuss the effect of each MHW definition based on data from the 1st 312 January 2014, during the event of the Pacific Blob (Fig. 6), we however note that our 313 descriptions are only from a single day, and may not represent longer term trends.

314 4.1 Baselines / climatologies

315 Baseline effect – Using the fixed WMO baseline yields lower percentile thresholds than a 316 climatology using later years (e.g. 1995 - 2024). As such, recent anomalies are more 317 frequently flagged as MHWs events, and with higher severity than when using warmer 318 climatological periods from later years, as evidenced from the Pacific Blob (Fig. 6,7).

319

320 Detrended effect – Removing each grid-cell's linear trend before building the climatology 321 reduces the warming signal embedded in the thresholds, as also discussed in Schlegel 322 et al., (2019). Globally, the share of MHWs was reduced when detrended SST is used, 323 compared to its non-detrended counterpart (Fig. 6), however, the effect was very minor for 324 the Pacific Blob (Fig. 7), indicating that the event was not attributed to long-term warming.

325

	No MHW (%)	MHW (%)	Category 1 (%)	Category 2 (%)	Category 3 (%)	Category 4 (%)
WMO90	93.4	6.6	5.2	0.9	0.3	0.2
Rean	93.8	6.2	5.0	0.7	0.3	0.1
WMO95	97.5	2.5	2.1	0.3	0.0	0.0
WMO99	99.5	0.5	0.5	0	0	0
detrended	94.6	5.4	4.3	0.7	0.3	0.1
Moving	91.3	8.7	6.9	1.2	0.3	0.2
Persisten-10	93.8	6.2	4.9	1	0.3	0.1
Persistent-30	97.4	2.6	1.6	0.7	0.3	0.1

Table 2: Summary statistics for area of oceans covered by MHWs alongside categories for different experiments.

328 4.2 Sensitivity to Threshold, Persistence and Detrending

Raising the percentile threshold or minimum duration acts as an increasingly strict filter on detections (Fig. 5/6). Generalised by assessing the 1st January 2014, we find that:



332

333

334

335 336

337

338

339

340

341

343 344

345

346

347

348

349

350

358

359

360

361

362 363

364

365

366

367

368 369

370

371

372 373



15

- Percentile effect Moving from the 90th to the 95th or 99th percentile progressively screened out moderate anomalies and highlighted only the strongest warm events (Fig. 6,7), and reduced the spatial extent and severity of events (Fig. 7C-D; Tab. 2).
- Duration effect Requiring 10 consecutive days (instead of 5) removed shorter MHWs, however only reduced MHW globally by 0.5% (Tab. 2). A 30-day minimum isolated only the most persistent basin-scale events globally (Fig. 6), and reduced the extent of MHWs by 4%. However, for the Pacific Blob there was little effect other than a slight reduction in the spatial extent of low-intensity areas (Fig. 7).
- Detrending effect After detrending, some events disappeared on a global scale (1.2% Tab. 2), making the threshold for MHW detection higher (Fig. 6). However, there was little effect on the Pacific Blob, which highlighted that the event was not due to long-term warming (Bond et al., 2014).
- Baseline choice (WMO vs Reanalysis) There was little difference on the global scale between the WMO and reanalysis baselines (0.4%, Tab. 2). However, the severity index for the Pacific Blob was generally higher for the WMO baseline than the reanalysis, with a greater extent of category 3 and 4 events (Fig. 7).
- Moving baseline (moving-average) A rolling 30-year climatology increased the
 occurrence of MHWs globally by 2.1% (Tab. 2). As the thresholds climb with time. As
 2014 is closer to the start of the rolling window, comparatively lower thresholds lead
 to greater MHW occurrences (Fig. 6).

351 Together, the panels show that the Blob's existence is robust across definitions, but its 352 spatial extent and intensity category vary depending on baseline, threshold and persistence 353 parameters.

5. Data Records and Access

355 All data described in this paper are archived in CF-compliant NetCDF format to facilitate 356 ease of use across programming languages and compliance with community standards. The 357 dataset is structured into several components:

- Daily Climatology files: These files contain the daily climatological percentiles for each grid cell under each baseline, each containing p10 and p50, and one of p90, p95, p99, depending on the experiment. The daily climatology files are also provided with threshold values for MHWs and MCSs. Each file is named by corresponding day-of-year, e.g. 362_Raw_90p_1991-2020_SSTCCI.nc.
- Anomaly files: We provide daily global maps of SST anomalies (difference above threshold), for both raw and detrended data, relative to both the fixed and moving climatologies. Daily files are provided for the entire data record, except for the moving averages and for p95 and p99 of the reanalysis period 1993-2016. For the moving averages, daily files are provided for only the last year in each window. Each file is named by corresponding date, e.g.
- 20161227 Raw 5d 90p 1991-2020 anomalies SSTCCI.nc.
- Category files: Categorical severities are provided for each day, encoding the MHW category (0 for none, 1–4 for moderate to extreme) based on the highest percentile threshold. In most of the experiments this is the 90th percentile threshold, though in select experiments we have computed categories based on the 95th and 99th





- percentile thresholds. (These latter thresholds often have many days of zero severity value since events are rarer at those levels). Daily files are provided for the entire data record, except for the moving averages and for p95 and p99 of the reanalysis period 1993-2016. For the moving averages, daily files are provided for only the last year in each window. Each file is named by corresponding date, e.g. 20161227 Raw 5d 90p 1991-2020 categories SSTCCI.nc.
- The folders are organised by input data source (in this case, only SSTCCI), whether the raw input has been used or it has been detrended first, the climatological period, the highest percentile used, and the duration of an event. E.g., the anomalies and categories for 10-day persistent events, calculated using the WMO climatological period with threshold p90, can be found at the path SSTCCI/Raw/WMO_Climatology/90p/duration/10_days/.

386 Each NetCDF file is accompanied by metadata attributes describing the variables, units, and 387 conventions, following CF (Climate and Forecast) standards. The data is publicly available at 388 https://download.dmi.dk/public/MHW and can also be accessed from the same location 389 using tools such as curl and wget.

6.Usage Notes

394

395

396

397

398

399

400 401

402

403

404

405

406

407

408

409 410

391 6.1 Potential Applications

392 This dataset is intended as a resource for a broad range of studies in oceanography, 393 climatology, and marine ecology. A few key applications include:

- Ecosystem impact studies: Researchers examining biological responses to ocean warming events can use the various MHW definitions to test sensitivity. For example, one could correlate coral bleaching occurrences or fishery yields with MHWs defined by the standard vs. a longer-duration criterion. If an impact (such as a coral bleaching event) correlates only with the longer, more intense MHWs, that insight could inform management, for example focusing on multi-week thermal stressors. Our detrended anomalies could also help separate impacts due to anomalous variability from those simply due to overall warming (Amaya et al., 2023).
- Climate model evaluation: Climate modellers can use the observational MHW statistics provided here to assess model skill. By applying the same algorithm to SST output from models (historical or future simulations), one can directly compare frequencies, durations, and intensities of MHWs between models and observations under consistent definitions. This is particularly useful given that different modeling studies have sometimes used different MHW thresholds; our dataset offers a common reference.

411 6.2 Code Availability

412 We aim to make this code available as a python package, for users to create their own 413 satellite-based MHW indicators, as such the code is currently under embargo.





7. Summary and Outlook

415 Here we have presented a comprehensive dataset that provides a flexible toolkit for studying 416 MHWs at the global scale. As this dataset enables direct comparisons of MHW 417 characteristics under different definitions, we address a critical need in the field, as divergent 418 definitions have made it difficult to compare results across studies. With our multi-definition 419 framework, researchers can now assess how much of the discrepancy between studies is 420 simply due to the choice of HMW definitions.

421 Through a brief analysis of our data, we showed that a short or moderate warming event 422 might be classified as an MHW under the less restrictive standard definition of a 90th 423 percentile and 5-day requirement, but would not register under a stricter definition (99th 424 percentile or 30-day minimum). Conversely, what we consider an "extreme" MHW under the 425 standard definition might be fairly routine under a shifting baseline in a warming climate. This 426 has implications for how we interpret long-term trends. Under a fixed baseline, there were 427 more MHWs than with a detrended baseline, consistent with the effect of climate change 428 driving more frequent extremes. Both fixed, moving, and detrended baselines are valid: the 429 fixed highlights the change relative to past climate, and the others highlights deviations from 430 the contemporary climate or long term warming. The dataset provides both views, and the 431 reality of ocean warming means users should be mindful of which dataset is most 432 appropriate for their studies. For example, whether the biological response of interest is 433 more sensitive to absolute temperatures or to deviations from a shifting mean, or whether an 434 event can truly be considered extreme if its occurrence has become increasingly frequent?

435 It is worth noting that while our dataset focuses on surface waters (being SST-based), 436 subsurface MHWs can also occur and may not always align with surface events. Our use of 437 SST CCI means areas of the ocean below the mixed layer are not directly assessed here. 438 Future efforts could merge this with subsurface temperature data or model output to 439 examine the vertical dimension of MHWs. Additionally, the framework here could be applied 440 to other variables (such as marine cold spells). The general approach of multi-definition 441 analysis is broadly applicable to extreme events research.

442 Looking ahead, we anticipate updating and expanding this dataset, adding new products and 443 definitions such as non-linear detrending as well as extending persistence thresholds for 444 detrended data. As new SST reanalysis products or satellite data become available, they 445 can be incorporated to extend the record and possibly improve accuracy in certain regions, 446 for example in coastal and sea ice covered areas. By embracing the complexity of definitions 447 rather than choosing a single metric, it enables a more nuanced understanding of extreme 448 ocean warming events under climate change.

449 8. Conclusions

450 Our global MHW dataset offers, in a single resource, daily data that span the spectrum of 451 commonly used definitions. As our dataset includes both fixed (1991-2020) and moving 452 30-year baselines, users can analyse how a warming-adjusted threshold reshapes event 453 counts relative to a historical climate normal. Parallel streams of raw and linearly detrended





454 SST anomalies further allow researchers to disentangle MHWs driven by natural variability 455 from those amplified by the long-term warming trend, an essential capability for attribution 456 studies. Event masks are provided at three intensity thresholds (90th, 95th and 99th 457 percentiles) and at three minimum-duration criteria (5, 10 and 30 consecutive days), 458 capturing everything from moderate, short-lived anomalies to the most persistent and 459 extreme episodes. By packaging these options side-by-side, the dataset becomes both a 460 practical tool for climate monitoring, ecosystem-impact assessment and model evaluation, 461 and a conceptual lens through which to examine how methodological choices alone can alter 462 our perception of ocean extremes. In short, the multi-definition design promotes transparent, 463 apples-to-apples comparisons across studies and supplies a robust foundation for deeper, 464 more nuanced understanding of MHWs in a rapidly changing climate.

465 Author contributions

466 All authors contributed to guiding the research process and provided scientific input
467 throughout. A.H., N.D., and M.R.P. generated the code and processed the data. A.H. wrote
468 the main manuscript text and prepared the figures. All authors (A.H., N.D., R.M., M.R.P.,
469 R.R., G.B., S.C., V.C., D.D., P.E., V.H., P.H., J.H., A.J.K., B.L., A.O., J.P., F.D.R., K.v.S., F.S.,
470 S.S., A.Z.R., S.O.) contributed to discussions, reviewed the manuscript, and provided
471 comments and revisions.

472 Disclaimer

473 NA

474 Competing Interests

475 There are no competing interests

476 Acknowledgements

477 We gratefully acknowledge the ESA Sea Surface Temperature Climate Change Initiative
478 (SST CCI) team for providing the satellite data used in this study. This work was supported
479 through the ObsSea4Clim project. We also thank the contributing institutes for their
480 collaboration, including the Danish Meteorological Institute (DMI), the Centro
481 Euro-Mediterraneo sui Cambiamenti Climatici (CMCC), the Nansen Environmental and
482 Remote Sensing Center (NERSC), the National Centre for Polar and Ocean Research
483 (NCPOR), the Spanish National Research Council (CSIC), the Hellenic Centre for Marine
484 Research (HCMR), the Finnish Meteorological Institute (FMI), the Nansen Environmental
485 Research Centre India (NERCI), +ATLANTIC CoLAB, Mercator Ocean International, and the
486 Laboratoire de Météorologie Dynamique (LMD).

487 References





- 488 Amaya, D. J., Alexander, M. A., Capotondi, A., Jacox, M. G., Gleckler, P. J., Lauvset, S. K., 489 ... Yeh, S.-W. (2023). Marine heatwaves need clear definitions so coastal communities can 490 adapt. *Nature*, 616(7955), 29–32. https://doi.org/10.1038/d41586-023-00924-2
- 491 Bond, N. A., Cronin, M. F., Freeland, H. J., & Mantua, N. J. (2015). Causes and impacts of 492 the 2014 warm anomaly in the NE Pacific. *Geophysical Research Letters*, 42(9), 3414–3420. 493 https://doi.org/10.1002/2015GL063306
- 494 Di Lorenzo, E., & Mantua, N. J. (2016). Multi-year persistence of the 2014/15 North Pacific 495 marine heatwave. *Nature Climate Change*, 6(11), 1042–1047. 496 https://doi.org/10.1038/nclimate3082
- 497 Donlon, C. J., Martin, M. J., Stark, J. D., Roberts-Jones, J., Fiedler, E., & Wimmer, W. 498 (2012). The Operational Sea Surface Temperature and Sea Ice Analysis (OSTIA) system. 499 *Remote Sensing of Environment, 116*, 140–158. https://doi.org/10.1016/j.rse.2010.10.017
- 500 Embury, O., Merchant, C. J., Good, S. A., Rayner, N. A., Høyer, J. L., Atkinson, C., Block, T.,
 501 Alerskans, E., Pearson, K. J., Worsfold, M., McCarroll, N., & Donlon, C. (2024).
 502 Satellite-based time-series of sea-surface temperature since 1980 for climate applications.
 503 Scientific Data, 11(1), 326. https://doi.org/10.1038/s41597-024-03147-w
- Frölicher, T. L., Fischer, E. M., & Gruber, N. (2018). Marine heatwaves under global warming.
 Nature, *560*(7718), 360–364. https://doi.org/10.1038/s41586-018-0383-9
- 506 Garrabou, J., Gómez-Gras, D., Medrano, Á., Cerrano, C., Ponti, M., Zuberer, F., ... Cebrián,
 507 E. (2019). A collaborative database to track mass mortality events in the Mediterranean Sea.
 508 Frontiers in Marine Science, 6, 707. https://doi.org/10.3389/fmars.2019.00707
- 509 Good, S. A., Fiedler, E., Mao, C., Martin, M. J., Maycock, A., Reid, R., ... Worsfold, M. 510 (2020). The current configuration of the OSTIA system for operational production of 511 foundation sea surface temperature and ice concentration analyses. *Remote Sensing*, 12(4), 512 720. https://doi.org/10.3390/rs12040720
- 513 Gonzalez, S., Sandvik, A. D., Jensen, M. F., Albretsen, J., Sandø, A. B., Ingvaldsen, R. B., 514 Hjøllo, S. S., & Vikebø, F. (2025). Drivers of the summer 2024 marine heatwave and record 515 salmon lice outbreak in northern Norway. *Communications Earth & Environment, 6*, 639. 516 https://doi.org/10.1038/s43247-025-02618-1
- 517 Hayward, A., Wright, S. W., Carroll, D., Law, C. S., Wongpan, P., Gutiérrez-Rodriguez, A., & 518 Pinkerton, M. H. (2025). Antarctic phytoplankton communities restructure under shifting 519 sea-ice regimes. *Nature Climate Change,* 15(8), 889–896. 520 https://doi.org/10.1038/s41558-025-02379-x
- 521 Hobday, A. J., Alexander, L. V., Perkins, S. E., Smale, D. A., Straub, S. C., Oliver, E. C. J., ... 522 Wernberg, T. (2016). A hierarchical approach to defining marine heatwaves. *Progress in Oceanography, 141*, 227–238. https://doi.org/10.1016/j.pocean.2015.12.014
- 524 Hobday, A. J., Oliver, E. C. J., Sen Gupta, A., Benthuysen, J. A., Burrows, M. T., Donat, M. 525 G., ... Smale, D. A. (2018). Categorizing and naming marine heatwaves. *Oceanography*, 526 31(2), 162–173. https://doi.org/10.5670/oceanog.2018.205



- 527 Macagga, N., & Hsu, J. (2025). Marine heatwaves and ocean acidification increase the risk 528 of coral bleaching in the Philippines. *Remote Sensing*, 17(5), 1022. 529 https://doi.org/10.3390/rs17051022
- 530 Jacobs, Z. L., Smale, D. A., Wernberg, T., Moore, P. J., & Sayer, M. D. J. (2024). Marine 531 heatwaves and cold spells in the Northeast Atlantic: What should the UK be prepared for?
- 532 Frontiers in Marine Science, 11, 1434365. https://doi.org/10.3389/fmars.2024.1434365
- 533 Lien, V. S., Raj, R. P., & Chatterjee, S. (2024). Surface and bottom marine heatwave 534 characteristics in the Barents Sea: A model study. *State of the Planet, 8*, 8. 535 https://doi.org/10.5194/sp-4-osr8-8-2024
- 536 Lonhart, S. I., Jeppesen, R., Beas-Luna, R., Crooks, J. A., & Raimondi, P. T. (2019). Shifts in 537 the distribution and abundance of coastal marine species along the eastern Pacific Ocean 538 during marine heatwaves from 2013 to 2018. *Marine Biodiversity Records, 12,* 13. 539 https://doi.org/10.1186/s41200-019-0171-8
- 540 Merchant, C. J., Embury, O., Bulgin, C. E., Block, T., Corlett, G. K., Fiedler, E., ... Donlon, C. 541 (2019). Satellite-based time-series of sea-surface temperature since 1981 for climate 542 applications. *Scientific Data*, *6*, 223. https://doi.org/10.1038/s41597-019-0236-x
- 543 Oliver, E. C. J., Donat, M. G., Burrows, M. T., Moore, P. J., Smale, D. A., Alexander, L. V., ... 544 Wernberg, T. (2018). Longer and more frequent marine heatwaves over the past century. 545 *Nature Communications*, *9*(1), 1324. https://doi.org/10.1038/s41467-018-03732-9
- 546 Pecuchet, L., Mohamed, B., Hayward, A., Alvera-Azcárate, A., Dörr, J., Filbee-Dexter, K., ...
 547 & Wernberg, T. (2025). Arctic and Subarctic marine heatwaves and their ecological impacts.
 548 Frontiers in Environmental Science, 13, 1473890.
 549 https://doi.org/10.3389/fenvs.2025.1473890
- 550 Purich, A., Doddridge, E.W. Record low Antarctic sea ice coverage indicates a new sea ice 551 state. *Commun Earth Environ* 4, 314 (2023). https://doi.org/10.1038/s43247-023-00961-9
- 552 Renner, H. M., Jones, T., Byrd, G. V., Hinke, J. T., & Kaler, R. S. A. (2024). Widespread 553 seabird mortality linked to a marine heatwave. *Science*, 384(6692), 747–752. 554 https://doi.org/10.1126/science.adq4330
- 555 Roberts, K. E., Allen, C. E., & Hawkins, S. J. (2019). Rockpool fish exhibit patterns of habitat 556 use and recruitment that are resilient to extreme warming events. *Marine Biology, 166*, 63. 557 https://doi.org/10.1007/s00227-019-3515-5
- 558 Schlegel, R. W., Oliver, E. C. J., Hobday, A. J., & Smit, A. J. (2019). Detecting marine 559 heatwaves with sub-optimal data. *Frontiers in Marine Science*, 6, 737. 560 https://doi.org/10.3389/fmars.2019.00737
- 561 Smale, D. A., Wernberg, T., Oliver, E. C. J., Thomsen, M., Harvey, B. P., Straub, S. C., ... 562 Moore, P. J. (2019). Marine heatwaves threaten global biodiversity and the provision of 563 ecosystem services. *Nature Climate Change*, 9(4), 306–312. 564 https://doi.org/10.1038/s41558-019-0412-1





- 565 Smith, K. E., Oliver, E. C. J., Smale, D. A., Wernberg, T., & Payne, B. L. (2025). Baseline 566 matters: Challenges and implications of different marine heatwave baselines. *Progress in Oceanography*, 231, 103404. https://doi.org/10.1016/j.pocean.2024.103404
- 568 Stroeve, J., Holland, M. M., Meier, W., Scambos, T., & Serreze, M. (2007). Arctic sea ice 569 decline: Faster than forecast. *Geophysical Research Letters*, 34(9). 570 https://doi.org/10.1029/2007GL029703
- 571 Wernberg, T., Bennett, S., Babcock, R. C., de Bettignies, T., Cure, K., Depczynski, M., ... 572 Wilson, S. (2016). Climate-driven regime shift of a temperate marine ecosystem. *Science*, 573 353(6295), 169–172. https://doi.org/10.1126/science.aad8745
- 574 World Meteorological Organization. (2023). *Guidelines on the definition and characterization* 575 of extreme weather and climate events (WMO-No. 1310). Geneva, Switzerland: WMO. 576 https://library.wmo.int/idurl/4/68271
- 577 Yang, C., Leonelli, F. E., Marullo, S., Artale, V., Beggs, H., Nardelli, B. B., ... Pisano, A. 578 (2021). Sea surface temperature intercomparison in the framework of the Copernicus 579 Climate Change Service (C3S). *Journal of Climate*, 34(13), 5257–5283. 580 https://doi.org/10.1175/JCLI-D-20-0793.1